A1/A2 lab information and exercise sheets

January 23, 2025

Contents

1 Introduction

There will be two formative online lab assessment tests taken via Blackboard in Aerodynamics 2. These notes give details of the lab exercises that you should undertake to prepare for these tests. Although the online tests are not compulsory, the material from the labs will be assessed during the final examination and the online tests are an excellent way to help prepare for that part of the exam.

2 Structure of lab exercises

There are two labs/exercises in this document:

1. A1 chordwise pressure ditribution lab - assessed as part of the A1 lab formative assessment test
2. A2 supersonic lab - assessed as part of the A2 lab formative assessment test

Please check the online pages for the staff responsible for the labs; they can help you resolve queries. For the lab exercises, please contact the postgraduate lab demonstrators by email in the first instance or speak to the academic staff after a lecture.

While staff endeavour to respond as swiftly as possible to emails, you will often find it quicker to to speak to us (the email inbox is a blunt tool!). There is nothing impolite about coming to ask us a question after a lecture; we prefer talking to typing.

Teaching of the A1 and A2 labs will consist of the following stages:

1. Lab demonstration with postgraduate demonstrator (during lab)
2. Discussion of lab learning prompts and lab sheet with postgraduate demonstrator (during lab)
3. Completion of learning exercises (during lab **and** own time)
4. Completion of the lab assessment test (1hr online BlackBoard test - precise timing will be notified)

Learning is structured so that all the material you will need to be familiar with for the lab assessment test is contained in this document.

The lab assessment test will not be a verbatim repetition of the lab sheet (ie. it will require you to show understanding of the learning prompts in different contexts), but if you have completed the lab sheet, and discussed anything you do not understand with the demonstrator or staff, this will be completely sufficient preparation to do well on the assessment test.

3 A1 laboratory exercise - chordwise pressure distribution on an aerofoil with a flap

The purpose of the A1 lab is to demonstrate typical aerofoil pressure distributions associated with a cambered aerofoil at varying angles of attack and flap deflection. If you have any queries in the first instance please check this document, and if that does not help, please contact the lab demonstrator or discuss with staff after a lecture.

3.1 Background

3.1.1 Introduction

When a body and a fluid stream are in relative motion, forces are generated on the surface of the body. On each elemental area of the surface, there is thus an elemental resultant force (section 5). It is conventional to consider this force in terms of two components: one normal to the local surface and one tangential to the local surface. The component normal to the local surface is expressed in terms of the pressure (local normal force divided by local area) and the component tangential to the local surface is expressed in terms of the shear stress (local shear force divided by local area).

In this experiment, the pressure distribution around an aerofoil is to be investigated. The pressure distribution is of great value in indicating the nature of the flow around the aerofoil: it will show stagnation points, regions of favourable and adverse pressure gradient (which affect the development of the boundary layer), regions susceptible to separation, and regions of actual separated flow. It also shows the distribution of pressure forces, and suitable integrations of these will give the overall forces and moments on the aerofoil due to the pressures. Details of how this can be done are given in section 5. Of particular note is the result that the normal force coefficient (the coefficient of the component of force normal to the chord line) is equal to the area enclosed by the graph of C_p against $\frac{x}{c}$. The major contribution to the normal force coefficient (and thus to the lift coefficient) is from negative pressure coefficients on the upper surface, and this is why pressure distributions for aerofoils are conventionally presented with the pressure coefficient negative upwards.

Let us consider how the forces and moments due to pressure differ from the total forces and moments such as would be measured on a balance. Usually pressures (or rather the difference from ambient pressure) are much greater than the shear stresses, and for an aerofoil shape, the thickness is much less than the chord. Thus for the normal force, the contribution of the shear stresses is extremely small (as it comes from the small shear stresses acting over a smaller resolved area), and so the normal force due to pressure is very close to the total normal force. For the chordwise force, the contribution of shear stresses is important, because although the shear stresses are smaller, they act over a larger resolved area. For the pitching moment and flap hinge moment, the integration of the moments of the pressure force components normal to the relevant chord line will give good results, as the moments of the chordwise forces, both those due to the pressure and those due to shear stress, are also extremely small because their moment arms are small.

The normal and chordwise force components can then be resolved to give lift and drag (which are the components perpendicular to, and in the direction of, the flow, section 5). For angles of incidence that are not too large, the lift coefficient is very close to the normal force coefficient, and thus the integrated pressure distribution gives a good indication of the total lift coefficient but the total drag has appreciable contributions both from the integrated pressures (the pressure drag or form drag), and from the integrated shear stresses (the skin friction drag).

Thus, a force balance can measure total drag, but pressure integration only gives pressure drag. Pressure drag at low speeds arises because the boundary layer modifies the pressure distribution such that the front and rear stagnation regions no longer cancel; primarily, the rear stagnation pressure is not recovered.

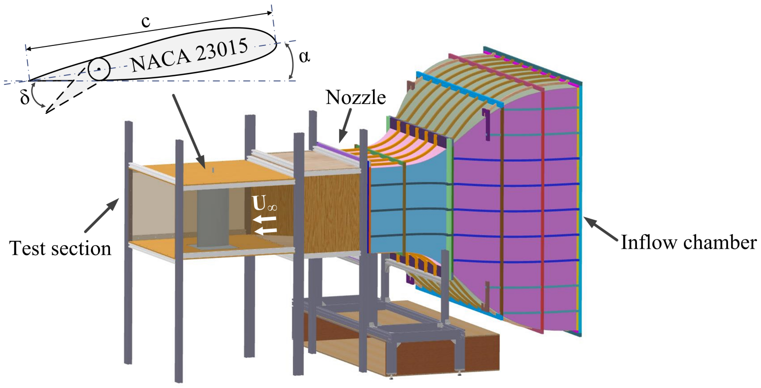

Figure 1: NACA 23015 aerofoil set-up in the low-speed wind tunnel

3.1.2 Objectives

The pressure distribution around a two-dimensional NACA 23015 aerofoil spanning a closed working section wind tunnel is to be measured using static pressure holes around the section at mid-span, for a series of values of incidence and flap deflection. For each pressure distribution the coefficients of lift, pressure drag, pitching moment and flap hinge moment can be calculated, and the variation of these with incidence and flap deflection is to be investigated.

Due to time restrictions, some data will be provided by the lab demonstrator.

3.1.3 Apparatus

- The closed-circuit open-jet low-speed wind tunnel at the Wind Tunnel Laboratory, see Figure 1.
- Two-dimensional NACA 23015 aerofoil with 30% hinged flap: static pressure tappings provided around the section at mid span. The positions of the tappings are shown in the spreadsheet. The incidence of the aerofoil can be altered, and also the angle of the flap relative to the aerofoil
- Pressures are measured by an electric pressure transducer, which is connected to each pressure tapping connection. A data acquisition system including data logger and computer records the pressure data. For each pressure distribution, the coefficients of lift, pressure drag, pitching moment and flap hinge moment are calculated

3.1.4 Procedure

The tunnel will be run at a wind speed of about 20ms^{-1}, which should be kept constant for all tests.

Investigate the pressure distribution for a range of incidence at zero flap angle. Do this initially without recording any data to obtain a feel for the different shapes of pressure distribution that occur. Observe that for a range of incidence near stall, two types of flow are possible, depending on whether the incidence is increased from an attached flow or decreased from a stalled flow condition (*i.e.*, hysteresis effects as discussed in the first recorded lecture). Obtain a set of results over an incidence range of -5^o to 25^o. Use intervals of 5^o at low angles, closer intervals of 2^o or less when characteristics are changing rapidly.

Obtain other sets of results showing the effects of varying the flap deflection. Observe that changing the flap deflection changes the pressure distribution over the whole aerofoil. Observe cases of flap angles of -10^o, 10^o,

20^o, 40^o and 60^o, all for an incidence of 10^o, but also obtain results which will enable you to discern the effect of varying flap deflection for other incidences, and the effect of different flap deflections on the variation with incidence. To obtain the attached flow condition for some flap deflections, you will probably have to start the tunnel with the incidence negative, and then set the required incidence with the tunnel running.

3.1.5 Spreadsheets

Required spreadsheets (available from the ”A1 and A2 labs” content area on blackboard:

- A1_Data_UG.xlsx - force and pressure data
- A1_SurfaceIntegration_UG.xlsx - template for performing force integral from pressure data

3.2 Learning prompts

These should be covered during the discussion session with your demonstrator. **You should make your notes in the space provided below so that when you come to prepare for the lab assessment test you have a ready-made set of revision notes**.

- What is the value of the Reynolds number at 20ms^{-1}?

- What is the value of the Mach number at 20ms^{-1}?

- What do these two non-dimensional numbers represent?

- What do the numbers in the NACA 23015 aerofoil designation mean?

- How does flap deflection influence the maximum C_l (the C_l at stall)? Why might this be useful?

- How does flap deflection influence stall angle?

- Illustrate with a diagram the regions of adverse and favourable pressure gradient. Will separation usually occur under an adverse or favourable pressure gradient?

- Where does the flow first separate from the aerofoil? What type of stall is this? Is the stall gradual or sudden? What would happen for a thinner section?

- How does the lift curve slope compare to the flat plate potential flow result of 2π/radian? List three potential reasons for the difference.

- Definition and usage of C_p

$$C_p = \frac{p - p_\infty}{\frac{1}{2}\rho V^2} \tag{1}$$

- Definition and usage of C_l, C_m and C_d

$$\begin{bmatrix} C_x \\ C_y \end{bmatrix} = \oint C_p \mathbf{n} d\left(\frac{s}{c}\right) \tag{2}$$

where $\mathbf{n}$ is the unit normal.

$$\begin{bmatrix} C_l \\ C_d \end{bmatrix} = \begin{bmatrix} \cos(\alpha) & -\sin(\alpha) \\ \sin(\alpha) & \cos(\alpha) \end{bmatrix} \begin{bmatrix} C_x \\ C_y \end{bmatrix} \tag{3}$$

$$C_m = \oint C_p \mathbf{n} \times \mathbf{d} d\left(\frac{s}{c}\right) = \oint C_p \begin{bmatrix} \Delta y \\ -\Delta x \end{bmatrix} \times \begin{bmatrix} x_m - x_{ref} \\ y_m - y_{ref} \end{bmatrix} d\left(\frac{s}{c}\right) \tag{4}$$

where $\mathbf{d}$ is the vector from the reference point to the location for that C_p value. Please also refer to section 5 in this document for more details. How would you find $C_{l,d,m}$ numerically from the experimental data (you will do this later using the data in the spreadsheet)?

- Sketch the influence of boundary layer transition on C_p vs. $\frac{x}{c}$

- Contributions to C_d come from skin friction and normal pressure forces. Which are measurable in this experiment? Why would it usually be unwise to measure C_d by surface integration?

- What effect do the wind tunnel walls have on $C_{l_{max}}$?

- The aerodynamic centre x_{ac} is the location about which pitching moments do not change with angle of attack, ie. $\frac{dC_{m_{AC}}}{d\alpha} = 0$

$$\begin{aligned} M_{LE} &= M_{AC} - Lx_{AC} \\ \frac{dC_{m_{LE}}}{d\alpha} &= -\frac{dC_l}{d\alpha}\frac{x_{AC}}{c} \end{aligned} \tag{5}$$

  Now calculate x_{ac} may be found - **The lab demonstrator will provide you with the values of the derivatives**.

- Calcula te the ratio of the projected frontal area of the aerofoil to the cross sectional area of the tunnel (0.6m x 0.6m) for small to high incidences. This is termed the blockage factor – is it acceptably small? What does this imply about measurements at larger incidences? Recall the aerofoil is 15% thick, and the chord is about 25cm

- How will flap deployment change the handling of an aircraft?

- What is hysteresis, what causes it and what does this imply for recovery of a stalled aircraft? Note that in free air hysteretic effects will be smaller than seen in the confined space of this wind tunnel owing to wall effects.

3.3 Learning exercises

- Plot C_l against α for all flap deflections in the spreadsheet. What happens to $\frac{dC_l}{d\alpha}$ as the flap angle is increased? What happens to $C_{l_{max}}$ and α_{stall} as the flap angle is increased?
- Plot C_p against $\frac{x}{c}$ for varying α. What happens to the suction peak as α is increased? What happens after stall?
- Plot:
  - C_p against $\frac{x}{c}$ for $\alpha = 5^o, \delta = 0^o, 5^o$ (ie. one graph with two lines)
  - C_p against $\frac{x}{c}$ for $\alpha = 10^o, \delta = 0^o, 20^o$ (ie. one graph with two lines)
  - C_p against $\frac{x}{c}$ for $\alpha = 20^o, \delta = 0^o, 40^o$ (ie. one graph with two lines)

  What does the flap do to the pressure curve? What has happened for $\alpha = 20^o$?
- Using the definitions in equations (2) and (3) calculate C_l and C_d for the pressure distribution in the spreadsheet (the cells you need to modify are shaded green). You will need to access the coordinates of the aerofoil from the Excel spreadsheet, and your integral may be programmed using a summation in the same spreadsheet. **Make sure you are familiar with the process before you leave the lab area**.

4 A2 laboratory exercise - supersonic flow on a double wedge aerofoil

The purpose of the A2 lab is to demonstrate typical aerofoil pressure distributions associated with a supersonic double wedge aerofoil at varying angles of attack and flap deflection, together with compressible nozzle behaviour.

4.1 Background

4.1.1 Introduction

This experiment is designed to give an opportunity of investigating the nature of the flow of supersonic air in a two dimensional nozzle and around aerofoils. Some of the results can be compared to theoretical prediction based on the assumptions of one-dimensional inviscid flow (as developed in the lecture course) and thus an indication of when these theoretical predictions are reasonably valid, and when they are misleading.

4.1.2 Apparatus

The wind tunnel (figure 2) works by induction. This means the ejection of a ‘small’ mass of high speed gas powers the continuous flow round the tunnel (this gives better run times than just using the high pressure gas). A downstream flow of compressed air induces (causes) an upstream airflow. This allows supersonic flow in a small (laboratory scale) tunnel with a smooth and controllable flow through the working section.

The user operates a valve to allow compressed air into the tunnel, just after the working section. A mechanical gauge and an electronic pressure transducer measure the inlet “reference” pressure. A special injector block directs the compressed air away and downstream from the working section, into a gradual expansion. The flow of compressed air downstream creates a pressure drop in the working section. Air moves round the duct and a contraction cone, then into the working section. This air flow leaves the working section, mixes with the compressed air flow and moves around the tunnel duct again in a cycle. Excess air leaves through the filter until the user shuts the compressed air valve. Three alloy blocks hold flow straighteners that smooth the flow, just upstream of the contraction cone.

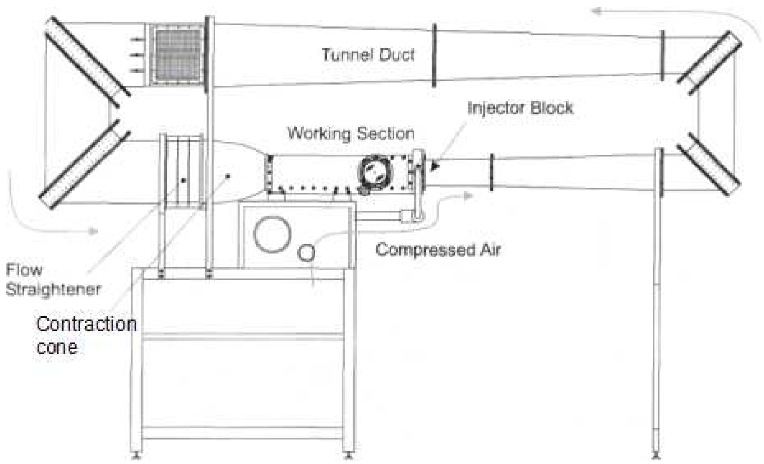

Figure 2: Supersonic ejector tunnel

Models fit into the working section (figure 3). Three interchangeable liners are available that provide different maximum Mach numbers in the working section. However, only the "Mach 1.8" liner will be used in these experiments. The working section has two circular glass windows ('portals'); each window is inside a gear ring. The models fit into the space between the windows. Slots in the windows hold the model in place. The user can turn a small angle control that turns the gear ring. This turns the angle of the portals and the model. An angle encoder on one side of the working section connects directly to the data acquisition system.

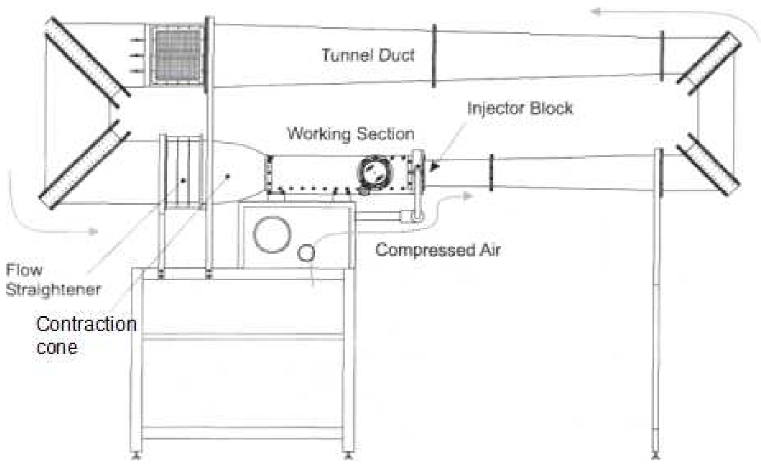

Figure 3: Tunnel working section

4.1.3 Schlieren system

Note: 'schlieren' is German for 'streaks' or 'slide', and should therefore not be capitalised (it is generally attributed in the form used here to August Toepler). It is also a placename in Austria but I am not aware of any connection. Shadowgraph images (eg. shadow of a candle on a wall) are produced by a different method to schlieren images, although they share some common usage and principles.

A schlieren system (figure 4) is provided for flow visualization. This is one of several optical techniques that make use of the fact that the speed of light in a gas decreases as the density increases, i.e. the refractive index is a function of density. The system used is shown in the diagram below. Light from a fairly small point source (discharge type of lamp, not monochromatic) is focused on a horizontal slit, which then acts as a line source of light. This is at the focal point of a lens (via a mirror), which then shines a parallel beam of light through the test section, perpendicular to the glass side walls. The light passes through a second lens that produces an image of the test section on the screen (again via a mirror). A horizontal knife-edge is introduced at the focal plane of the second lens, where there is an image of the horizontal line source. This cuts off part of the light reaching the screen, and thus reduces the level of illumination there. This cut in light intensity should still be uniform however (for no gas flow) as the knife-edge is at the focal point of the mirror.

When there is a flow in the nozzle, then a strong density gradient in a direction perpendicular both to the light beam and to the knife-edge will cause the light to be refracted perpendicular to the knife-edge. Depending on the sign of the gradient, more or less light will be cut off by the knife-edge, and corresponding parts of the image of the flow on the screen will be darker or lighter. Features of the flow, which can be seen because of their strong density gradients, include shock waves, expansion waves and boundary layers. (Shock waves appear as dark lines with the system shown).

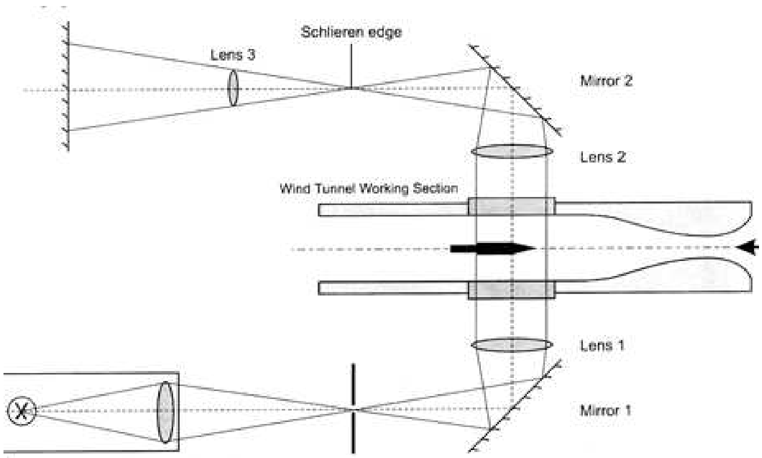

Figure 4: Schlieren system

4.1.4 Digital data acquisition system

The lower wall of the wind tunnel working section has 25 equispaced static pressure tappings. Two static pressure tappings (labelled 26 & 27) are placed on the upper surface of a 10^o double-wedge aerofoil. A further pitot pressure probe (28) is placed in the contraction. Each of these pressure tappings is connected to a digital pressure transducer that allows data acquisition software on an attached PC to automatically collect a time series of simultaneous pressure measurements. The data acquisition software also simultaneously records the model angle, the reference (supply) pressure and the atmospheric pressure.

When dealing with compressible flow, all pressures should be absolute pressures. The data acquisition software gives pressures relative to atmosphere and this must be accounted for. Static pressures should be calculated in coefficient form as a ratio of total, i.e. $\frac{p}{p_0}$. This can be done using the upstream pitot pressure reading, taken in the contraction, as the total pressure relative to atmosphere.

The data acquisition software allows the data to be partially processed and displayed, however it is easier to place the results into the excel spreadsheet provided (A2_Data_UG.xlsx). This spreadsheet also calculates and plots a number of results useful for the report.

4.1.5 Hydraulic analogy

The main features of the real two-dimensional flow of a gas can be demonstrated qualitatively by making use of the approximate analogy that exists with the flow of a liquid with a free surface in an open channel, so a water table will be used for demonstation purposes. Flows in a convergent-divergent nozzle will be demonstrated, and also features of other supersonic flows.

The water channel apparatus consists of a horizontal glass surface over which the water flows, with a constant-head pump supplying water to one end, and an adjustable weir controlling the height of the water at the downstream end.

The basis of the hydraulic analogy can be seen by considering the equations of mass flow and energy for one-dimensional flows.

For gas flow in a two-dimensional nozzle, conservation of mass flow gives

$$\rho b u = \text{constant} \tag{6}$$

where b is the width of the nozzle, whereas for the water flow,

$$hbu = \text{constant} \tag{7}$$

where h is the height of the water.

Thus the height of the water is analogous to the density of the gas. The energy equation for an adiabatic gas flow is

$$C_P T + \frac{u^2}{2} = \text{constant} \tag{8}$$

whereas for a no-loss water flow,

$$gh + \frac{u^2}{2} = \text{constant} \tag{9}$$

Thus for isentropic flow, the height of the water is analogous to the temperature of the gas as well.

Consider the relationship $p/\rho = RT$ for compressible flow. Using the assumptions previously stated, this can be written as $p/h = Rh$, ie. $p = Rh^2$.

For isentropic flow, $p =$ constant $\times\ \rho^\gamma$. By comparing, a value of $\gamma = 2$ is implied. Hence the analogy is only approximate for a gas such as air with $\gamma = 1.4$, and has further errors for flows with viscous dissipation, such as shock waves.

The speed of sound in a gas is the speed of propagation of small pressure disturbances. Thus in the water flow, this is analogous to the speed of propagation of small height disturbances, i.e. surface gravity waves. Thus flows analogous to subsonic and supersonic flows in a gas can be set up in the water flow, depending on whether the speed of the water flow is less than or greater than the speed of propagation of surface gravity waves (for surface waves, the Froude number is largely analogous to the Mach number, and is used in hydraulics).

4.1.6 Procedure

Pressure measurements should be taken to form the basis of observations. After use of the compressible flow theory developed in the lectures quantities such as Mach number and pressure coefficient can be calculated.

For each of the tests a reference pressure of approximately 8bar will give the longest running time. Higher pressures will not increase the maximum Mach number, just reduce the run time. Once the reference pressure drops below 8bar quickly shut off the supply valve.

Before opening the supply valve start the timed data recording using the data acquisition software, and stop it shortly after shutting the supply valve at the end of the test. After each test, examine the pressure data; there will be a number of sets of data for different times in the test. Choose a set of data for a reference pressure near 8bar that is steady, the rest of the data can be removed. Before the next test always remember to open a new data set. After completing all the tests described below export the results to an html file. This allows the data to be copied and pasted in the A2_Data_UG.xlsx spreadsheet.

The following tests should be run:

1. Record all relevant data without a model in the portal
2. Place the 5^o single wedge aerofoil into the portal slots, blunt edge into flow. Observe and record the bow shock displayed by the schlieren system as well as all relevant pressure data
3. Place the pressure tapped 10^o double wedge aerofoil into the portal slots
   (a) Estimate the model zero angle of attack. As the flow in the nozzle is not purely one-dimensional and the nozzle is not symmetrical, the onset flow is not parallel to the working section floor

(b) For a number of model incidences between the maximum and minimum, observe and record the oblique shock and expansion waves displayed by the schlieren system. Simultaneously record all relevant pressure data. Steps in incidence of approximately 2^o is sufficient, apart from around 0^o where steps of 1^o should be taken

4.1.7 Spreadsheets

Required spreadsheets:

- A2_WedgeAerofoil_UG.xlsx - pressure calculations for double wedge aerofoils
- A2_Data_UG.xlsx - data and post-processing

4.2 Learning prompts

These should be covered during the discussion session with your demonstrator. **You should make your notes in the space provided below so that when you come to prepare for the lab assessment test you have a ready-made set of revision notes**.

- What effect does the model have on flow upstream of it? Are there any exceptions?

- Why do the shocks as viewed on the schlieren screen have an apparent substantial thickness?

- Why do the trailing edge shocks appear more diffuse than the leading edge?

- How closely do the measured and calculated pressures and Mach numbers along the tunnel wall match one dimensional theory? What causes the differences?

- Why do the pressure coefficients not match the theory at high/low angles of attack, especially on the front surface? What causes this? Sketch the flow structure in this situation. Using compressible tables estimate the angle for which this flow structure should form, and suggest why the angles are different to this in the experiment

- In the hydraulic analogy, what represents density? What represents temperature? What represents pressure?

4.3 Learning exercises

- Using the wedge aerofoil spreadsheet compute the theoretical C_p values on the front and rear faces of the upper surface for all measured angles of attack (the Mach number at the model location can be found from the wall data spreadsheet; it will be about 1.7 to 1.8). Plot these theoretical C_p values and the experimental ones on the same graph against α. Why does the aft surface pressure coefficient not match the theoretical predictions when the forward surface results do? (In other words, why is the offset between theory and experiment different for the forward and aft surfaces?

- Why may the angle of attack measured be inaccurate? How can we measure this inaccuracy using tunnel geometry, C_p values or C_l? Estimate the angle offset for this experiment using each approach.

- What maximum pressure coefficient would be expected on the forward surface of the blunt body? What assumption is needed, and how accurate would we expect it to be?

5 Force Coefficients

Note: this section is repeated from the tips and tricks document for convenience here.

If the arc length along the surface of the aerofoil is s, then considering a small element of length ds on the surface of the aerofoil the pressure force acts in the inward normal direction and has magnitude $dF = pds$. Then if $\mathbf{n}$ is the inward pointing unit normal (points towards the inside of the aerofoil, magnitude unity) then the vector force on the element of the aerofoil surface is given by $d\mathbf{F} = p\mathbf{n}ds$. To obtain, $\mathbf{F}$, the total vector force per unit depth on an aerofoil from pressure (i.e. ignoring viscous shear stresses) we integrate around the aerofoil surface as follows:

$$\mathbf{F} = \oint_{aerofoil} p\mathbf{n}ds = \int_0^{s_{max}} p\mathbf{n}ds \tag{10}$$

where s_{max} is the arc length of the curve defining the aerofoil surface. Note that p is not a variable we like to work with; C_p is preferable. So

$$p = C_p q_\infty + p_\infty \tag{11}$$

where q_∞ is dynamic pressure. So

$$\mathbf{F} = \oint_{aerofoil} \left(C_p q_\infty + p_\infty\right) \mathbf{n}ds \tag{12}$$

A constant pressure integrated around the boundary generates no lift, so this is the same as

$$\mathbf{F} = \oint_{aerofoil} C_p q_\infty \mathbf{n}ds \tag{13}$$

Finally it is usual to work with dimensionless force coefficients rather than forces hence dividing through by $q_\infty c$ gives

$$\mathbf{C}_F = \frac{\mathbf{F}}{q_\infty c} = \oint_{aerofoil} C_p \mathbf{n} d\left(\frac{s}{c}\right) \tag{14}$$

where c is chord and $\mathbf{C}_F = (C_X, C_Y)$, where C_X, C_Y are the non-dimensional force coefficients in the x and y directions respectively given by

$$C_X = \oint_{aerofoil} C_p \mathbf{n} \cdot \mathbf{i} d\left(\frac{s}{c}\right) \tag{15}$$

$$C_Y = \oint_{aerofoil} C_p \mathbf{n} \cdot \mathbf{j} d\left(\frac{s}{c}\right) \tag{16}$$

Now if we have a straight small element of the surface of length ds then if we move around the surface in a clockwise manner then the inward unit normal is given by

$$\mathbf{n} = \left(\frac{dy}{ds}, -\frac{dx}{ds}\right) \tag{17}$$

Note that $ds = \sqrt{dx^2 + dy^2}$. If you unsure of why this is the form of the unit normal vector note that a vector along the element is (dx, dy) and if you dot product this with the unit normal above you get zero as they are perpendicular. You can show it has length 1. Then the force coefficient equations become

$$C_X = \oint_{aerofoil} C_p d\left(\frac{y}{c}\right) \tag{18}$$

$$C_Y = -\oint_{aerofoil} C_p d\left(\frac{x}{c}\right) \tag{19}$$

Then for cases when the surface of the aerofoil is represented as a series of N flat panels a discrete form of these equations can be used, where the contribution to the corresponding force coefficent from each face is summed to get the total force coefficient as follows

$$C_X = \sum_{i=1}^{i=N} C_{X_i} = \sum_{i=1}^{i=N} C_{p_i} \frac{\Delta y_i}{c} \tag{20}$$

$$C_Y = \sum_{i=1}^{i=N} C_{Y_i} = -\sum_{i=1}^{i=N} C_{p_i} \frac{\Delta x_i}{c} \tag{21}$$

where the summation is over all the straight panels representing the aerofoil. These are simply summations of C_p multiplied by the projected areas of the straight segments in each axis direction. Interestingly, because the shock-expansion theory used in this part of the course gives a constant pressure on any straight line segment, these summations are the exact integrals, with no error. This is not true for subsonic flow where the smooth variations in pressure will introduce an error in the integrals.

However, this is not quite what we want still, as C_L and C_D are defined relative to the flow vector at ∞, so we need to rotate through α

$$C_L = C_Y \cos(\alpha) - C_X \sin(\alpha) \tag{22}$$

$$C_D = C_Y \sin(\alpha) + C_X \cos(\alpha) \tag{23}$$

As an exercise you may want to show that

$$C_M = \sum_{i=1}^{i=N} C_{p_i} \frac{\Delta y_i}{c} \frac{(y_{mid_i} - y_{ref})}{c} + \sum_{i=1}^{i=N} C_{p_i} \frac{\Delta x_i}{c} \frac{(x_{mid_i} - x_{ref})}{c} \tag{24}$$

about (x_{ref}, y_{ref}) where nose-up is positive and (x_{mid}, y_{mid}) is the mid point of a straight segment. Commonly $(x_{ref}, y_{ref}) = (0.25c, 0.0)$, but $(0, 0)$ and $(0.5c, 0)$ are also used. These three are commonly used since $(0.25c, 0.0)$ is the incompressible aerodynamic centre, $(0.5c, 0.0)$ is the compressible aerodynamic centre, and $(0, 0)$ is just convenient as it normally refers to the leading edge.

Notes
1) If we move around the surface in an anticlockwise manner (i.e. integrate anticlockwise around the surface) then the inward unit normal is given by $\mathbf{n} = \left(-\frac{dy}{ds}, \frac{dx}{ds}\right)$ and hence the expressions obtained for the force coefficients C_X and C_Y will thus have opposite signs to those found above.
2) If the aerofoil has been non-dimensionalised so that the chord is 1 then we can drop c from all the above equations for force and moment coefficients.